RAA 2019 Vol. **19** No. **6**, 85(8pp) doi: 10.1088/1674–4527/19/6/85
© 2019 National Astronomical Observatories, CAS and IOP Publishing Ltd.
http://www.raa-journal.org *http://iopscience.iop.org/raa*

Research in Astronomy and Astrophysics

IU Cancri: a solar-type contact binary with mass transfer

Hui-Yu Yuan[1], Hai-Feng Dai[2] and Yuan-Gui Yang[2]

[1] Information College, Huaibei Normal University, Huaibei 235000, China
[2] School of Physics and Electronic Information, Huaibei Normal University, Huaibei 235000, China; *yygcn@163.com*

Received 2018 December 28; accepted 2019 January 29

Abstract We present new CCD photometry of the solar-type contact binary IU Cnc, which was observed from November 2017 to March 2018 with three small telescopes in China. BV light curves imply that IU Cnc is a W-type contact binary with total eclipses. The photometric solution indicates that the mass ratio and fill-out factor are $q = 4.104 \pm 0.004$ and $f = 30.2\% \pm 0.3\%$, respectively. From all available light minimum times, the orbital period may increase at a rate of $dP/dt = +6.93(4) \times 10^{-7}\,\mathrm{d\,yr^{-1}}$, which may result from mass transfer from the secondary component to the primary one. With mass transferring, IU Cnc may evolve from a contact configuration into a semi-detached configuration.

Key words: binaries: close — binaries: eclipsing — stars: individual (IU Cancri)

1 INTRODUCTION

Eclipsing binaries are key objects for study, which can provide fundamental stellar properties and critical tests on the theories of stellar evolution and structure. The theory of thermal relaxation oscillations (see the review by Webbink 2003) postulates that a binary system can oscillate between contact and semi-detached states. Orbital period variations may provide some straightforward information, such as mass transfer and loss, and magnetic activity, and reveal an additional companion body around the binary star. Recently, the spectra of contact binaries, included in the LAMOST[1] (Luo et al. 2015) database, were statistically analyzed by Qian et al. (2017). Therefore, it is necessary to monitor some binary systems at special stages, which may provide some key observational evidence on the formation and evolution of contact binaries.

IU Cnc [$\alpha_{J2000.0} = 09^{\rm h}00^{\rm m}59.06^{\rm s}$, $\delta_{J2000.0} = +12^\circ58'51.87''$] is an EW-type binary identified from the Northern Sky Variability Survey (Woźniak et al. 2004). Its light variability ranges from 11.80 mag to 12.36 mag. Kreiner (2004) determined an orbital period of 0.4216450 d, which was later updated to 0.4216475 d (Otero & Wils 2005). This short-period eclipsing binary was then successively listed in three catalogs derived from sky surveys (Avvakumova et al. 2013; Drake et al. 2014; Huber et al. 2016). From *Gaia* Data Release 2, the absolute stellar parallax for IU Cnc is 2.0684 ± 0.0422 mas (Gaia Collaboration 2018), which determines a distance of 483.5 ± 9.9 pc from Earth. Three spectra of IU Cnc are obtained from the LAMOST survey, which are displayed in Figure 1. The flare around the Hα line that was recorded on 2017 April 15 may be unremoved cosmic rays.

The spectral information is listed in Table 1. The associated phases are computed by the epoch of the observed primary eclipse, HJD 2458080.3572 (see Table 4). From this table, the spectral type of the more massive component (i.e., the primary) should be G2, because its observed phase (i.e., 0.869) only approaches the primary eclipse, indicating it is a W-type contact binary (see Sect. 3). Except for several light minimum times, no photometry or period analysis for this solar-type binary IU Cnc has been published up to now.

2 CCD PHOTOMETRY

New photometry of IU Cnc was acquired from November 2017 to March 2018, by employing the 80-cm telescope (Zheng et al. 2008) and the 85-cm telescope (Zhou et al. 2009) at Xinglong Station (XLS) of National Astronomical Observatories, Chinese Academy of Sciences (NAOC), and the 1.0-m telescope operated by Yunnan Astronomical Observatories (YNAO). These three telescopes are equipped with the standard Johnson

[1] `http://www.lamost.org`

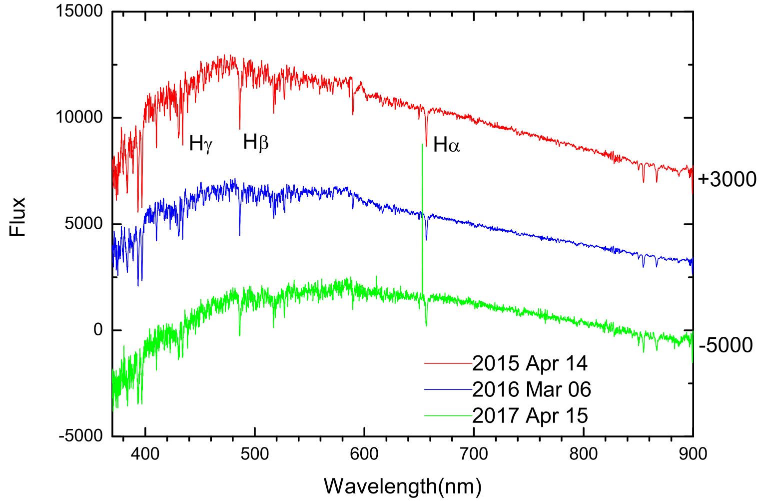

Fig. 1 The low-precision spectra of IU Cnc, which were observed by LAMOST from 2015 to 2017.

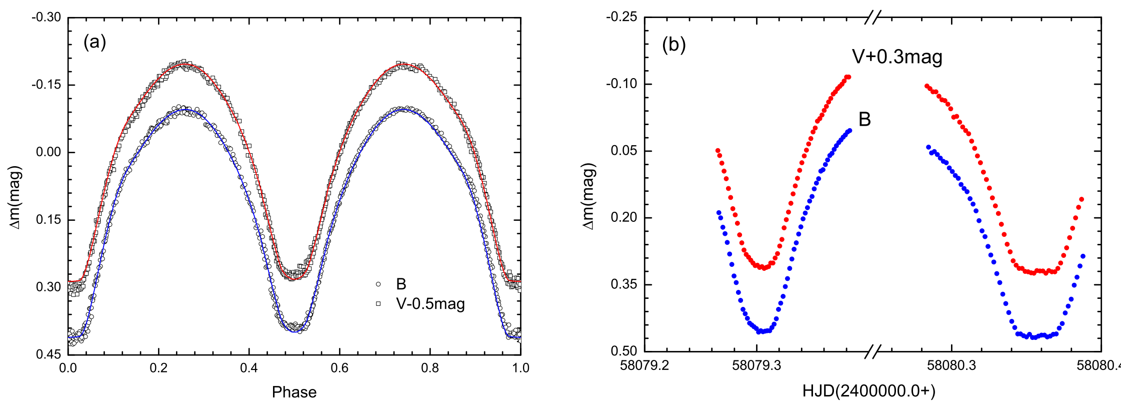

Fig. 2 The complete light curves (a) and two eclipse times (b) for IU Cnc, which were observed in 2018 by several small telescopes. The continuous lines are constructed by the photometric solution.

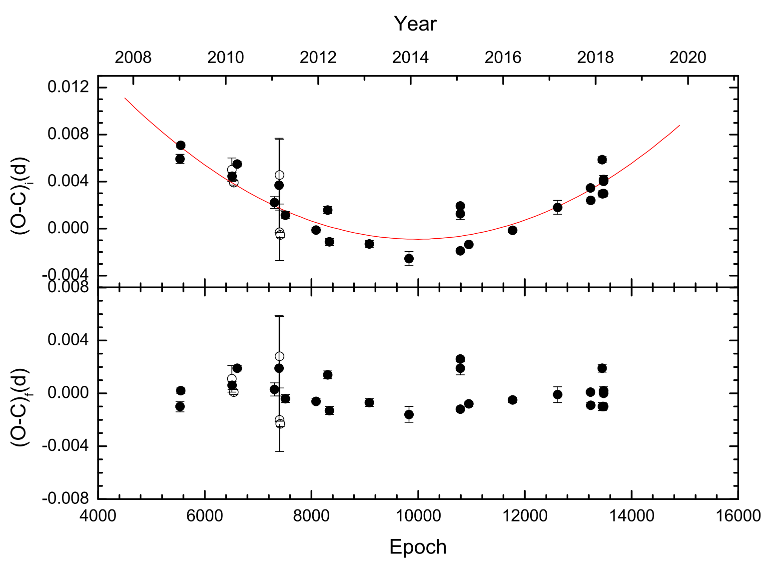

Fig. 3 Residuals of $(O-C)_i$ (*upper panel*) and $(O-C)_f$ (*lower panel*) for IU Cnc. The *solid line* is plotted by Eq. (2). The *filled* and *open circles* refer to photoelectric and CCD measurements, respectively.

Table 1 The Spectral Information from LAMOST

No.	Median JD (Hel.)	Sp.	$T_{\rm eff}$	$\log(g)$	[Fe/H]	Phase[a]
1	2457127.0542	F9	6099 ± 14 K	4.123 ± 0.022	0.172 ± 0.012	0.597
2	2457454.4847	G2	6076 ± 21 K	4.265 ± 0.035	0.217 ± 0.019	0.357
3	2457989.0604	G2	6074 ± 118 K	3.985 ± 0.193	0.218 ± 0.114	0.869

Notes: [a] Phases correspond to the primary eclipse time (i.e., HJD 2458080.3572) at the epoch T_0 with an orbital period of 0.42164408 d (see Eq. (1) of Sect. 3).

Table 2 Observing Log for the Contact Binary IU Cnc

No.	Observing Date	Exposure time	Data Number	Standard Error	Telescope
1	2017 Nov. 21, 22	70 s (B), 60 s (V)	113(B), 113 (V)	0.003mag (B), 0.003 mag (V)	80-cm (XLS)
2	2018 Feb. 22, 23, 25	50 s (B), 40 s (V)	308(B), 332 (V)	0.013mag (B), 0.009 mag (V)	1.0-m (YNAO)
3	2018 Mar. 04, 05	50 s (B), 40 s (V)	269(B), 262 (V)	0.006mag (B), 0.017 mag (V)	85-cm (XLS)

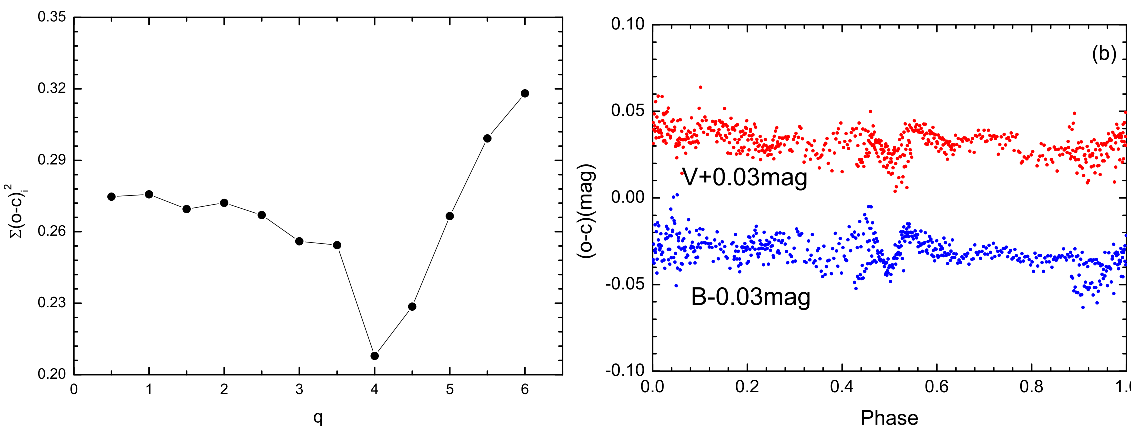

Fig. 4 (a) The relation between q and Σ, which is deduced from our BV light curves. (b) Residuals $(o-c)$ of the observed light curves.

$UBVR_cI_c$ filters. All photometric reductions were carried out by using IRAF in standard mode, including bias and dark subtraction, and flat-field correction.

In the observing process, TYC 817-2361-1 ($V = 11.21 \pm 0.11$ mag) and TYC 817-2308-1 ($V = 11.43 \pm 0.12$ mag) were chosen as comparison and check stars, respectively. Detailed information about the observations is given in Table 2. The typical exposure times depended on weather. The standard error is determined by the magnitude difference between the comparison and check stars. The individual differential magnitudes (i.e., $\Delta m = m_{\rm var} - m_{\rm comp}$) with their associated Heliocentric Julian Dates (i.e., HJDs) in 2018 are listed in Table 3. The complete light curves, i.e., 577 data in B and 594 data in V, are displayed in the left panel of Figure 2, and the corresponding phases are computed by Equation (1) (see Sect. 3). The amplitudes of variable light are 0.472 mag in B and 0.506 mag in V bands. Two eclipses are shown in the right panel of Figure 2. From this figure, the primary eclipse is a total one with a duration of 37 min, implying that IU Cnc is a W-type contact binary. This kind of total eclipse occurs in other contact binaries, such as V343 Ori (Yang et al. 2008), AS CrB (Liu et al. 2017) and EF Dra (Yang 2012). The long duration of the total eclipse indicates that the mass ratio may be small or orbital inclination is large. From our new data, we determined several light minimum times, which are written in Table 4.

3 INCREASING ORBITAL PERIOD

For the eclipsing binary IU Cnc, no period analysis has been performed up till now. From the $O - C$ gateway[2], we compiled all eclipse times together with seven newly observed ones.

Table 5 provides 24 available light minimum times, including five photoelectric and 19 CCD measurements. With the weights from observed errors, we update a new ephemeris as follows,

$$\begin{aligned} {\rm Min.I} = {\rm HJD}\ 2452500.1058(20) \\ + 0.42164408(23) \times E\ , \end{aligned} \quad (1)$$

[2] http://var2.astro.cz/ocgate/

Table 3 Photometric Observations of IU Cnc in 2018

B band				V band			
JD (Hel.)	Δm	JD (Hel.)	Δm	JD (Hel.)	Δm	JD (Hel.)	Δm
2458172.2283	+0.055	2458175.3279	−0.080	2458172.2254	+0.448	2458175.3031	+0.359
2458172.2294	+0.061	2458175.3291	−0.091	2458172.2266	+0.463	2458175.3042	+0.362
2458172.2306	+0.061	2458175.3302	−0.087	2458172.2277	+0.451	2458175.3054	+0.354
2458172.2317	+0.071	2458175.3313	−0.090	2458172.2289	+0.475	2458175.3065	+0.349
2458172.2328	+0.076	2458175.3336	−0.095	2458172.2300	+0.485	2458175.3076	+0.349
2458172.2341	+0.085	2458175.3347	−0.088	2458172.2311	+0.498	2458175.3088	+0.344
2458172.2352	+0.105	2458175.3359	−0.099	2458172.2323	+0.479	2458175.3099	+0.343
2458172.2364	+0.104	2458175.3370	−0.090	2458172.2334	+0.479	2458175.3111	+0.348
2458172.2375	+0.115	2458175.3393	−0.086	2458172.2347	+0.496	2458175.3122	+0.348
2458172.2386	+0.118	2458175.3404	−0.096	2458172.2358	+0.502	2458175.3133	+0.330
2458172.2398	+0.141	2458175.3415	−0.097	2458172.2369	+0.512	2458175.3145	+0.330
2458172.2409	+0.155	2458182.1655	+0.312	2458172.2381	+0.522	2458175.3157	+0.338
2458172.2421	+0.163	2458182.1673	+0.328	2458172.2392	+0.527	2458175.3168	+0.331
2458172.2432	+0.174	2458182.1686	+0.347	2458172.2403	+0.550	2458175.3180	+0.318
2458172.2443	+0.187	2458182.1699	+0.340	2458172.2415	+0.556	2458175.3191	+0.324
2458172.2455	+0.202	2458182.1711	+0.363	2458172.2426	+0.555	2458175.3202	+0.318
2458172.2466	+0.215	2458182.1724	+0.371	2458172.2437	+0.568	2458175.3214	+0.322
2458172.2477	+0.221	2458182.1737	+0.381	2458172.2449	+0.593	2458175.3225	+0.316
2458172.2489	+0.238	2458182.1749	+0.378	2458172.2460	+0.599	2458175.3237	+0.315
2458172.2500	+0.251	2458182.1762	+0.379	2458172.2472	+0.618	2458175.3248	+0.305
2458172.2511	+0.255	2458182.1775	+0.384	2458172.2483	+0.624	2458175.3259	+0.309
2458172.2523	+0.275	2458182.1788	+0.390	2458172.2494	+0.632	2458175.3273	+0.307
2458172.2534	+0.293	2458182.1801	+0.389	2458172.2506	+0.653	2458175.3285	+0.305
2458172.2546	+0.304	2458182.1813	+0.389	2458172.2517	+0.661	2458175.3296	+0.308
2458172.2557	+0.322	2458182.1826	+0.391	2458172.2528	+0.673	2458175.3308	+0.306
2458172.2568	+0.331	2458182.1839	+0.394	2458172.2540	+0.680	2458182.1666	+0.710
2458172.2582	+0.346	2458182.1851	+0.390	2458172.2551	+0.703	2458182.1679	+0.723
2458172.2593	+0.362	2458182.1864	+0.385	2458172.2562	+0.711	2458182.1692	+0.735
2458172.2605	+0.360	2458182.1877	+0.390	2458172.2574	+0.722	2458182.1705	+0.747
2458172.2616	+0.387	2458182.1890	+0.392	2458172.2588	+0.744	2458182.1717	+0.757
2458172.2628	+0.385	2458182.1902	+0.398	2458172.2599	+0.748	2458182.1730	+0.761
2458172.2639	+0.383	2458182.1915	+0.390	2458172.2610	+0.755	2458182.1743	+0.767
2458172.2650	+0.402	2458182.1928	+0.392	2458172.2622	+0.772	2458182.1755	+0.771
2458172.2662	+0.383	2458182.1941	+0.390	2458172.2633	+0.775	2458182.1768	+0.763
2458172.2684	+0.408	2458182.1953	+0.391	2458172.2644	+0.779	2458182.1781	+0.775
2458172.2696	+0.401	2458182.1966	+0.382	2458172.2656	+0.782	2458182.1794	+0.775
2458172.2709	+0.404	2458182.1979	+0.381	2458172.2667	+0.765	2458182.1806	+0.771
2458172.2720	+0.404	2458182.1992	+0.368	2458172.2678	+0.774	2458182.1819	+0.781
2458172.2731	+0.409	2458182.2004	+0.360	2458172.2701	+0.785	2458182.1832	+0.781
2458172.2743	+0.395	2458182.2017	+0.346	2458172.2714	+0.779	2458182.1845	+0.779
2458172.2754	+0.411	2458182.2030	+0.339	2458172.2726	+0.792	2458182.1858	+0.777
2458172.2768	+0.402	2458182.2043	+0.323	2458172.2737	+0.778	2458182.1870	+0.772
2458172.2779	+0.405	2458182.2055	+0.311	2458172.2748	+0.780	2458182.1883	+0.768
2458172.2791	+0.410	2458182.2081	+0.288	2458172.2760	+0.788	2458182.1896	+0.778
2458172.2802	+0.411	2458182.2094	+0.270	2458172.2773	+0.788	2458182.1908	+0.767
2458172.2813	+0.405	2458182.2106	+0.253	2458172.2785	+0.797	2458182.1921	+0.768
2458172.2825	+0.416	2458182.2119	+0.236	2458172.2796	+0.796	2458182.1934	+0.771
2458172.2836	+0.413	2458182.2132	+0.237	2458172.2819	+0.796	2458182.1947	+0.762
2458172.2847	+0.419	2458182.2144	+0.214	2458172.2830	+0.792	2458182.1959	+0.765
2458172.2859	+0.403	2458182.2157	+0.204	2458172.2842	+0.796	2458182.1972	+0.754
2458172.2881	+0.398	2458182.2170	+0.197	2458172.2853	+0.794	2458182.1985	+0.745
2458172.2893	+0.416	2458182.2183	+0.176	2458172.2864	+0.801	2458182.1998	+0.740
2458172.2904	+0.410	2458182.2195	+0.171	2458172.2876	+0.804	2458182.2010	+0.730
2458172.2916	+0.392	2458182.2208	+0.163	2458172.2887	+0.804	2458182.2023	+0.723
2458172.2927	+0.383	2458182.2221	+0.151	2458172.2898	+0.793	2458182.2036	+0.706
2458172.2938	+0.379	2458182.2234	+0.140	2458172.2910	+0.784	2458182.2049	+0.691
2458172.2950	+0.385	2458182.2246	+0.122	2458172.2921	+0.781	2458182.2074	+0.688
2458172.2961	+0.360	2458182.2259	+0.117	2458172.2932	+0.769	2458182.2087	+0.669
2458172.2972	+0.347	2458182.2272	+0.113	2458172.2944	+0.765	2458182.2100	+0.657
2458172.2984	+0.322	2458182.2284	+0.095	2458172.2955	+0.755	2458182.2112	+0.645
2458172.2995	+0.320	2458182.2297	+0.093	2458172.2966	+0.746	2458182.2125	+0.631
2458172.3006	+0.320	2458182.2310	+0.084	2458172.2978	+0.726	2458182.2138	+0.620
2458172.3018	+0.294	2458182.2323	+0.075	2458172.2989	+0.708	2458182.2150	+0.603
2458172.3029	+0.285	2458182.2336	+0.073	2458172.3001	+0.703	2458182.2163	+0.590
2458172.3040	+0.285	2458182.2348	+0.063	2458172.3012	+0.696	2458182.2176	+0.575
2458172.3052	+0.274	2458182.2361	+0.049	2458172.3023	+0.683	2458182.2189	+0.564
2458172.3063	+0.255	2458182.2374	+0.042	2458172.3035	+0.651	2458182.2201	+0.555
2458172.3075	+0.253	2458182.2386	+0.040	2458172.3046	+0.654	2458182.2214	+0.550
...	...	...	... ...	...	...	...	...

Notes: The full table is available online (`http://www.raa-journal.org/docs/Supp/ms4331_Table3.pdf`).

Table 4 Newly Obtained Light Minimum Times

JD (Hel.)	Min	Error	Filter	Telescope
2458079.30405	II	±0.00096	B	80-cm (XLS)
2458079.30417	II	±0.00012	V	80-cm (XLS)
2458080.35715	I	±0.00022	B	80-cm (XLS)
2458080.35722	I	±0.00023	V	80-cm (XLS)
2458172.27926	I	±0.00024	B	1.0-m (YNAO)
2458172.27817	I	±0.00027	V	1.0-m (YNAO)
2458173.33024	I	±0.00023	B	1.0-m (YNAO)
2458173.33064	I	±0.00029	V	1.0-m (YNAO)
2458182.18545	II	±0.00025	B	85-cm (XLS)
2458182.18455	II	±0.00021	V	85-cm (XLS)
2458183.02942	II	±0.00017	B	85-cm (XLS)
2458183.02924	II	±0.00016	V	85-cm (XLS)
2458183.24069	I	±0.00036	B	85-cm (XLS)
2458183.23985	I	±0.00027	V	85-cm (XLS)

Table 5 All Compiled Eclipse Times for IU Cnc

JD (Hel.)	Error	Method	Epoch	Min	$(O-C)_i$ (d)	$(O-C)_f$ (d)	Reference
2454833.9050	±0.0004	CCD	5535.0	I	+0.0059	−0.0010	[1]
2454839.8092	±0.0002	CCD	5549.0	I	+0.0071	+0.0002	[1]
2455244.3755	±0.0010	pe	6508.5	II	+0.0050	+0.0011	[2]
2455245.8507	±0.0003	CCD	6512.0	I	+0.0045	+0.0006	[3]
2455260.3969	±0.0002	pe	6546.5	II	+0.0039	+0.0001	[2]
2455286.3297	±0.0002	CCD	6608.0	I	+0.0055	+0.0019	[4]
2455580.8454	±0.0005	CCD	7306.5	II	+0.0022	+0.0003	[5]
2455617.3192	±0.0040	CCD	7393.0	I	+0.0037	+0.0019	[6]
2455621.3208	±0.0024	pe	7402.5	II	−0.0003	−0.0020	[2]
2455621.5365	±0.0030	pe	7403.0	I	+0.0046	+0.0028	[2]
2455626.3803	±0.0002	pe	7414.5	II	−0.0006	−0.0023	[7]
2455667.7032	±0.0003	CCD	7512.5	II	+0.0011	−0.0004	[5]
2455909.9370	±0.0002	CCD	8087.0	I	−0.0001	−0.0006	[8]
2456002.7006	±0.0003	CCD	8307.0	I	+0.0016	+0.0014	[9]
2456015.3472	±0.0003	CCD	8337.0	I	−0.0011	−0.0013	[6]
2456330.5267	±0.0003	CCD	9084.5	II	−0.0013	−0.0007	[10]
2456643.5968	±0.0006	CCD	9827.0	I	−0.0026	−0.0016	[11]
2457049.4309	±0.0001	CCD	10789.5	II	−0.0019	−0.0012	[12]
2457049.6448	±0.0005	CCD	10790.0	I	+0.0013	+0.0019	[12]
2457050.4888	±0.0001	CCD	10792.0	I	+0.0019	+0.0026	[12]
2457117.3162	±0.0002	CCD	10950.5	II	−0.0013	−0.0008	[12]
2457463.6988	±0.0002	CCD	11772.0	I	−0.0001	−0.0005	[13]
2457820.2016	±0.0000	CCD	12617.5	II	+0.0018	−0.0001	[14]
2458079.3041	±0.0001	CCD	13232.0	I	+0.0035	+0.0001	[15]
2458080.3572	±0.0002	CCD	13234.5	II	+0.0024	−0.0009	[15]
2458172.2792	±0.0003	CCD	13452.5	II	+0.0059	+0.0019	[15]
2458173.3304	±0.0003	CCD	13455.0	I	+0.0030	−0.0010	[15]
2458182.1850	±0.0002	CCD	13476.0	I	+0.0030	−0.0010	[15]
2458183.0293	±0.0002	CCD	13478.0	I	+0.0040	+0.0000	[15]
2458183.2403	±0.0003	CCD	13478.5	II	+0.0042	+0.0002	[15]

References: [1] Diethelm 2009; [2] Hubscher et al. 2012; [3] Diethelm 2010 [4] Brat et al. 2011; [5] Diethelm 2011; [6] Hoňková et al. 2013; [7] Hubscher & Lehmann 2012; [8] Nelson 2012; [9] Diethelm 2012; [10] Honková et al. 2014; [11] Honkova et al. 2015; [12] Juryšek et al. 2017; [13] Nelson 2017; [14] Nagai 2018; [15] This Study.

whose standard derivation in a parenthesis is in the unit of the last decimal place. The residuals, $(O-C)_i$, are listed in Table 5. The corresponding $O-C$ curve is displayed in the upper panel of Figure 3. From this figure, the orbital period apparently shows a secular increase. A linear least-squares solution with weights leads to the following equation,

$$(O-C)_i = 0.0330(1) - 7.53(1) \times 10^{-6} E + 4.004(2) \times 10^{-10} E^2 \ . \qquad (2)$$

Table 6 Photometric Elements of the Contact Binary IU Cnc

Parameter	Star 1 (Sec.)	Star 2 (Pri.)
$q = M_2/M_1$	4.014 ± 0.004	
$i(^\circ)$	80.43 ± 0.12	
T (K)	6272 ± 4	6075 ± 118^a
A	0.5	0.5
g	0.32	0.32
X, Y	+0.649, +0.218	+0.649, +0.217
x_B, y_B	+0.831, +0.182	+0.832, +0.179
x_V, y_V	+0.751, +0.254	+0.752, +0.252
Ω	7.7395 ± 0.0053	
$^b\ell_{iB}$	0.2618 ± 0.0006	0.7382 ± 0.0015
ℓ_{iV}	0.2523 ± 0.0006	0.7477 ± 0.0018
$r_{\rm pole}$	0.2595 ± 0.0013	0.4810 ± 0.0020
$r_{\rm side}$	0.2717 ± 0.0014	0.5230 ± 0.0023
$r_{\rm back}$	0.3152 ± 0.0017	0.5505 ± 0.0029
$\Sigma(O-C)_i^2$	0.8587	
f	$30.2 \pm 0.3\%$	

Notes: ^{a} The mean effective temperature for Star 2 (i.e., the primary component) is taken from the LAMOST data. ^{b} $\ell_i = L_i/(L_1 + L_2)$.

Table 7 Several W-type Contact Binaries with Increasing Period

Star	Sp.	$q^{\rm a}$	Period (d)	dP/dt ($\times 10^{-7}$ d yr^{-1})	f (%)	Reference
EQ Cep	-	0.526	0.30695	11.7	62.1	Liu et al. (2011)
AD Cnc	K0V	0.770	0.28274	4.94	8.3	Qian et al. (2007)
IU Cnc	G2	0.249	0.42164	6.93	30.2	Present study
V1191 Cyg		0.107	0.31338	4.5	68.6	Zhu et al. (2011)
CE Leo	K	0.533	0.30343	3.05	15.8	Yang et al. (2013)
GU Ori	G0V	0.455	0.47068	1.45	26.9	Yang et al. (2017)
BB Peg	F8V	0.370	0.36150	0.30	34	Kalomeni et al. (2007)
V432 Per	G4V	0.374	0.38331	1.19	3.3	Lee et al. (2008)

Notes: ^{a} The mass ratio is $q = M_{\rm s}/M_{\rm p}$, where $M_{\rm p}$ and $M_{\rm s}$ are the masses for the primary and secondary components, respectively.

The final residuals, $(O-C)_f$, are also listed in Table 5, and are plotted in the lower panel of Figure 3. From the quadratic coefficient of Equation (2), we can easily determine a period increase rate of $dP/dt = +6.93(4) \times 10^{-7}\,{\rm d\,yr^{-1}}$.

4 PHOTOMETRIC SOLUTION

On five nights in February and March of 2018, we first obtained two-color light curves, which are used to derive the photometric solution by the 2015 version of the Wilson-Devinney Code[3] (Wilson & Devinney 1971; Wilson & van Hamme 2016). As displayed in the left panel of Figure 2, IU Cnc is a total contact binary, whose geometric elements are reliable only from light curves. In the calculation, the limb darkening, gravity darkening, and albedo coefficients are taken from the literature (van Hamme 1993; Lucy 1967; Ruciński 1973). The adjustable parameters are listed as follows: T_1, $\Omega_{1,2}$, L_1 and q.

The spectra of IU Cnc are displayed in Figure 1, whose phases are given in Table 1. For the W-subtype binary seen in Figure 2(a), the more massive component (i.e., the primary) is occulted by the less massive one (i.e., the secondary) at a deep eclipse time (i.e., zero phase). The observed spectrum should be attributed to radiation from the primary component. Therefore, the spectral type of the primary is G2. Its mean effective temperature of $T_{\rm p} = 6075 \pm 120$ K is taken from Table 1. Moreover, the spectral type of F9 may result from the spectrum being polluted by the secondary component.

Due to lack of a mass ratio, we first preformed a series of solutions deduced from BV light curves. The mass ratio ranges from 0.5 to 6.0 with a step of 0.5. The contact configuration is always assumed. The resulting residuals versus mass ratio (i.e., Σ and q) are displayed in Figure 4(a), where a minimum value of Σ occurs around $q = 4$. This in-

[3] *ftp://ftp.astro.ufl.edu/pub/wilson/lcdc2015*

dicates that IU Cnc is a W-subtype contact binary. Then we consider q as a free parameter. The final photometric solution is derived and listed in Table 6. The calculated light curves are shown in Figure 2(a) as solid lines. Their corresponding residuals $(o-c)$ (i.e., observed values minus theoretical ones), are displayed in Figure 4(b). Although small distortions still exist around phase 0.5, the overall trend of BV observations is described by our photometric solution very well. This may be similar to another previously studied binary, WW Gem (Yang et al. 2014). The fill-out factor for this binary is $f = 30.2\% \pm 0.3\%$.

5 DISCUSSION

According to the spectral type of G2 for IU Cnc, the mass of the primary is adopted to be $M_{\rm p} = 1.0(\pm 0.02)\, M_\odot$ (Drilling & Landolt 2000), but the associated error depends on the uncertainty of its effective temperature. Combined with the photometric elements in Table 6, other absolute parameters for IU Cnc are given as follows, $M_{\rm s} = 0.25(\pm 0.08)\, M_\odot$, $R_{\rm p} = 1.36(\pm 0.11)\, R_\odot$, $R_{\rm s} = 0.74(\pm 0.06)\, R_\odot$, $L_{\rm p} = 2.24(\pm 0.35)\, L_\odot$, and $L_{\rm s} = 0.75(\pm 0.11)\, L_\odot$.

The orbital period of IU Cnc may be undergoing a secular increase as described by Equation (2). This situation appears in other W-type contact binaries, which are listed in Table 7. From this table, the period increase rate is typical for this kind of binary. The period increase may generally be attributed to mass transfer from the less massive component to the more massive one. Assuming conservative transfer, its mass transfer rate may be computed by the following equation (Singh & Chaubey 1986),

$$\frac{\dot{P}}{P} = 3\frac{1-q}{q}\frac{\dot{M}_{\rm p}}{M_{\rm p}}\,, \tag{3}$$

where the mass ratio is $q = M_{\rm s}/M_{\rm p}$. Inserting $\dot{P}$, P, q and $M_{\rm p}$ into Equation (3), the rate of mass transfer is $dM_{\rm p}/dt = +1.82(\pm 0.01) \times 10^{-7}\, M_\odot\,{\rm yr}^{-1}$. This will result in the mass ratio increasing with mass transfer, which causes the inner and outer critical Lagrangian surfaces to inflate. Finally, the Roche lobe of such a binary system approximates the inner critical Lagrangian surface. In this case, the binary will evolve into a "broken-contact" configuration as predicted by the thermal relaxation model (Webbink 2003).

Therefore, IU Cnct provides more good observational evidence supporting the thermal relaxation oscillation model (TRO; Webbink 2003), and resembles other binaries, such as DD Com (Zhu et al. 2010), II Per (Zhu et al. 2009), RV Psc (He & Qian 2009) and UU Lyn (Zhu et al. 2007).

In future observations, it will be necessary to obtain radial velocity curves and more eclipse times for IU Cnc in order to determine the absolute parameters and to identify the orbital period increase.

Acknowledgements All authors express thanks to the referee for his/her helpful comments. This research has received funding from the National Natural Science Foundation of China (Nos. 11873003 and 11473009), the Natural Science Research Project (No. KJ 2017A850) and the Outstanding Young Talents Program (No. gxyq2018161) of the Educational Department of Anhui Province. New photometry of IU Cnc is performed by using 80-cm and 85-cm telescopes at the XLS of NAOC. This work was partially supported by the Open Project Program of the Key Laboratory of Optical Astronomy, National Astronomical Observatories, Chinese Academy of Sciences.

References

Avvakumova, E. A., Malkov, O. Y., & Kniazev, A. Y. 2013, Astronomische Nachrichten, 334, 860
Brat, L., Trnka, J., Smelcer, L., et al. 2011, Open European Journal on Variable Stars, 137, 1
Diethelm, R. 2009, Information Bulletin on Variable Stars, 5894, 1
Diethelm, R. 2010, Information Bulletin on Variable Stars, 5945, 1
Diethelm, R. 2011, Information Bulletin on Variable Stars, 5992, 1
Diethelm, R. 2012, Information Bulletin on Variable Stars, 6029, 1
Drake, A. J., Graham, M. J., Djorgovski, S. G., et al. 2014, ApJS, 213, 9
Drilling, J. S., & Landolt, A. U. 2000, Normal Stars, ed. A. N. Cox, Allen's Astrophysical Quantities, ed. A. N. Cox (New York: AIP Press) 381
Gaia Collaboration, 2018, A&A, 616, A1
He, J., & Qian, S. 2009, Ap&SS, 321, 209
Honková, K., Juryšek, J., Lehký, M., et al. 2014, Open European Journal on Variable Stars, 165, 1
Honkova, K., Jurysek, J., Lehky, M., et al. 2015, Open European Journal on Variable Stars, 168, 1
Hoňková, K., Juryšek, J., Lehký, M., et al. 2013, Open European Journal on Variable Stars, 160, 1
Huber, D., Bryson, S. T., Haas, M. R., et al. 2016, ApJS, 224, 2
Hubscher, J., & Lehmann, P. B. 2012, Information Bulletin on Variable Stars, 6026, 1

Hubscher, J., Lehmann, P. B., & Walter, F. 2012, Information Bulletin on Variable Stars, 6010, 1

Juryšek, J., Hoňková, K., Šmelcer, L., et al. 2017, Open European Journal on Variable Stars, 179, 1

Kalomeni, B., Yakut, K., Keskin, V., et al. 2007, AJ, 134, 642

Kreiner, J. M. 2004, Acta Astronomica, 54, 207

Lee, J. W., Youn, J.-H., Kim, C.-H., Lee, C.-U., & Kim, H.-I. 2008, AJ, 135, 1523

Liu, L., Qian, S.-B., Zhu, L.-Y., et al. 2011, MNRAS, 415, 3006

Liu, L., Qian, S., Zhu, L., et al. 2017, New Astron., 51, 1

Lucy, L. B. 1967, ZAp, 65, 89

Luo, A.-L., Zhao, Y.-H., Zhao, G., et al. 2015, RAA (Research in Astronomy and Astrophysics), 15, 1095

Nagai, K., 2018, Var. Star Bull. Japane Stars, 64, 1, `http://vsolj.cetus-net.org/vsoljno64.pdf`

Nelson, R. H. 2012, Information Bulletin on Variable Stars, 6018, 1

Nelson, R. H. 2017, Information Bulletin on Variable Stars, 6195, 1

Otero, S. A., & Wils, P. 2005, Information Bulletin on Variable Stars, 5630, 1

Qian, S.-B., Yuan, J.-Z., Soonthornthum, B., et al. 2007, ApJ, 671, 811

Qian, S.-B., He, J.-J., Zhang, J., et al. 2017, RAA (Research in Astronomy and Astrophysics), 17, 087

Ruciński, S. M. 1973, Acta Astronomica, 23, 79

Singh, M., & Chaubey, U. S. 1986, Ap&SS, 124, 389

van Hamme, W. 1993, AJ, 106, 2096

Webbink, R. F. 2003, in Astronomical Society of the Pacific Conference Series, 293, 3D Stellar Evolution, eds. S. Turcotte, S. C. Keller, & R. M. Cavallo, 76

Wilson, R. E., & Devinney, E. J. 1971, ApJ, 166, 605

Wilson, R. E., & van Hamme, Computing Binary Star Observables, 2016, Florida International University, `http://faculty.fiu.edu/~vanhamme/wdfiles/ebdoc2016-bf.pdf`

Woźniak, P. R., Vestrand, W. T., Akerlof, C. W., et al. 2004, AJ, 127, 2436

Yang, Y.-G. 2012, RAA (Research in Astronomy and Astrophysics), 12, 419

Yang, Y.-G., Wei, J.-Y., & He, J.-J. 2008, AJ, 136, 594

Yang, Y.-G., Dai, H.-F., & Zhang, J.-F. 2013, New Astron., 19, 27

Yang, Y.-G., Yang, Y., Dai, H.-F., & Yin, X.-G. 2014, AJ, 148, 90

Yang, Y., Dai, H., Yuan, H., Zhang, X., & Zhang, L. 2017, PASJ, 69, 69

Zheng, W.-K., Deng, J.-S., Zhai, M., et al. 2008, ChJAA (Chin. J. Astron. Astrophys.), 8, 693

Zhou, A.-Y., Jiang, X.-J., Zhang, Y.-P., & Wei, J.-Y. 2009, RAA (Research in Astronomy and Astrophysics), 9, 349

Zhu, L.-Y., Qian, S.-B., Boonrucksar, S., He, J.-J., & Yuan, J.-Z. 2007, ChJAA (Chin. J. Astron. Astrophys.), 7, 251

Zhu, L. Y., Qian, S. B., Zola, S., & Kreiner, J. M. 2009, AJ, 137, 3574

Zhu, L., Qian, S.-B., Mikulášek, Z., et al. 2010, AJ, 140, 215

Zhu, L. Y., Qian, S. B., Soonthornthum, B., He, J. J., & Liu, L. 2011, AJ, 142, 124